Journal of Hazardous Materials 161 (2009) 848–853

Contents lists available at ScienceDirect

Journal of Hazardous Materials

journal homepage: www.elsevier.com/locate/jhazmat

Magnetic γ-Fe_2O_3 nanoparticles coated with poly-L-cysteine for chelation of As(III), Cu(II), Cd(II), Ni(II), Pb(II) and Zn(II)

Brianna R. White, Brandon T. Stackhouse, James A. Holcombe*

Department of Chemistry and Biochemistry, University of Texas at Austin, Austin, TX 78712, United States

ARTICLE INFO

Article history:
Received 1 February 2008
Received in revised form 8 April 2008
Accepted 9 April 2008
Available online 3 May 2008

Keywords:
Magnetic nanoparticle
Iron oxide
Metal binding peptide
Poly-L-cysteine
Metal remediation

ABSTRACT

Poly-L-cysteine ($PLCys_n$) ($n = 20$) was immobilized onto the surface of commercially available magnetic γ-Fe_2O_3 nanoparticles, and its use as a *selective* heavy metal chelator was demonstrated. Magnetic nanoparticles are an ideal support because they have a large surface area and can easily be retrieved from an aqueous solution. $PLCys_n$ functionalization was confirmed using FTIR and the quantitative Ellman's test. Metal binding capacities for As(III), Cd(II), Cu(II), Ni(II), Pb(II) and Zn(II) were determined at pH 7.0 and compared to adsorption capacities for unfunctionalized γ-Fe_2O_3 nanoparticles. The effect of pH on the $PLCys_n$ functionalized nanoparticles was also investigated. For all of the metals examined, binding capacities (μmol metal/g support) were more than an order of magnitude higher than those obtained for $PLCys_n$ on traditional supports. For As(III), Cu(II), Ni(II) and Zn(II), the binding capacities were also higher than the metal adsorption capacities of the unfunctionalized particles. Metal uptake was determined to be rapid (<2.5 min) and metal recoveries of >50% were obtained for all of the metals except As(III). $PLCys_n$, which has a general metal selectivity towards soft metals acids, was chosen to demonstrate the proof of concept. Greater metal selectivity may be achievable through the use of combinatorial peptide library screening or by using peptide fragments based on known metal binding proteins.

1. Introduction

Remediation of heavy metal ions from contaminated areas has become a significant area of research due to the severe risks they pose for human health and the environment [1]. The development of novel systems for remediation and preconcentration is required because unlike organic pollutants, metals can be a recirculating contaminant [2,3] and cannot be metabolized or decomposed. A recent advancement in metal remediation and extraction has been the exploration of peptides immobilized onto solid supports [4]. In biological systems, the tertiary structure of metal binding proteins is responsible for the formation of size selective cavities, but this tertiary structure is frequently lost once the proteins are removed from their pristine cellular environment [5]. Short chain synthetic peptides are more durable than natural proteins due to the *absence of a preformed structure*, allowing the peptide backbone to "wrap" around a metal as it binds. This allows for fast binding kinetics, which is an improvement over some metal chelators such as crown ethers [6]. Additionally, the metal can be released "on demand" by simply lowering the pH, which alters the peptide's structure [7].

These immobilized peptides have also demonstrated high metal binding capacities and frequently exhibit metal selectivity, which is due to the side group functionality of the amino acid(s) [4]. In particular, the biohomopolymer poly-L-cysteine ($PLCys_n$) (Fig. 1) has been shown to be an effective metal chelator in aqueous solution [8–12]. It preferentially and strongly ($\log K_f > 12$) binds soft metal acids such as Cd^{2+} and Pb^{2+} through its soft donor ligand thiol side groups [13]. As a result, $PLCys_n$ has successfully been used as an ion-exchange system for the remediation of soft acid metals while immobilized on a variety of supports such as glassy carbon electrodes [14], control pore glass [9–11], membranes [15,16] and graphite powder [12].

While many functionalized resin materials and support media with immobilized chelators are used in flow-through column applications, bulk remediation using chelator-attached support is another alternative. This approach frequently presents two short comings: slow binding because of mass transport constraints and inefficient and/or slow removal of support media from the aqueous waste stream after metal extraction.

This research considers the incorporation of ferromagnetic, Fe_2O_3 nanoparticles as the support media for immobilized $PLCys_n$. Filtration or centrifugation is typically used for macroscopic support removal. However, studies have shown these methods are not as selective, efficient or rapid as using a magnetic field to collect

* Corresponding author. Tel.: +1 512 471 5140; fax: +1 512 471 0985.
E-mail address: holcombe@mail.utexas.edu (J.A. Holcombe).

0304-3894/$ – see front matter © 2008 Elsevier B.V. All rights reserved.
doi:10.1016/j.jhazmat.2008.04.105

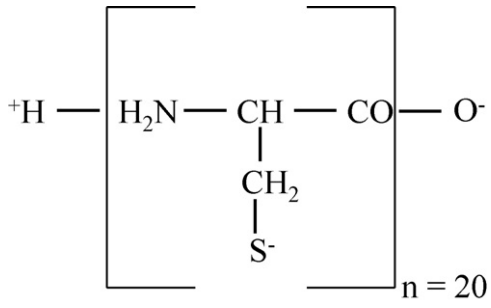

Fig. 1. Structure of poly-L-cysteine.

ferromagnetic particles [17–19]. Furthermore, common supports such as resin beads, porous glasses and carbon-based powders have diameters in the μm–mm range. If one considers "nanometer particles" in the range of 10–100 nm diameter and more conventional media in the 10–1000 μm range; for a given mass of media, the particle density increase with the nanoparticles falling between 10^6 and 10^{15}. For mass transport limited binding kinetics, a proportionate increase in extraction is to be expected. Additional speed is also gained since slower diffusional transport to the interior of the macroparticles is needed to access the binding sites within the particles. In contrast, binding is limited to the surface of nanoparticles. If one ignores interior sites, simply decreasing the size of the particles from micrometers to nanometers for a given mass of media increases the amount of available metal binding surface area by 100–1000 times [20].

Unfunctionalized iron oxide has been used previously as a metal adsorber [20–23], but control of metal selectivity was limited, and the interactions between the iron oxide and metal were often irreversible [23,24]. Additionally, other species such as phosphates also adsorb well and can out-compete metals for sorption sites due to their high concentrations in ground water [25].

In this study, we have immobilized $PLCys_n$ onto the surface of commercially available magnetic γ-Fe_2O_3 nanoparticles. Attaching $PLCys_n$ to the surface of the nanoparticle should allow the metal chelating system to benefit from the selectivity of the peptide motif. Also, the $PLCys_n$ surface coverage may also protect the nanoparticles from acid attack and thus permit acid stripping of the loaded particles so that they can be reused after the target metals are reclaimed. The binding affinity of the $PLCys_n$–Fe_2O_3 nanoparticles (PLCys–Nano) to the metals Cu(II), Cd(II), Ni(II), Pb(II) and Zn(II) were tested due to their known affinities for $PLCys_n$ from previous studies [9–11] As(III) binding was also investigated because of its extreme toxicity [26,27] mobility, and its propensity to bind sulfur groups in essential proteins [28,29].

2. Experimental

2.1. Reagents

All chemicals were reagent grade unless noted, and deionized distilled water was used to prepare solutions. All glassware and plasticware were soaked overnight in 4 mol L^{-1} HNO_3 prior to use. Peptide synthesis reagents Wang resin (100–200 mesh, 1.2 mmol g^{-1}), cysteine (Fmoc-Cys(Trt)-OH) and 2-(1*H*-benzotriazole-1-yl)-1,1,3,3-tetramethylaminium hexafluorophosphate (HBTU) were used as received from Novabiochem. Metal containing solutions were prepared by dilution from 1000 μg mL^{-1} stock solutions. A 0.05 mol L^{-1} (*N*-[hydroxyethyl]piperazine-*N*′-[2-ethanesulfonic acid]) (HEPES) (Sigma–Aldrich) buffer was prepared and adjusted to pH 7.0 with ammonium hydroxide (Fisher Scientific). Other reagents used include toluene (99.8%) (Acros), (3-aminopropyl)triethoxysilane (98%), trifluoroacetic acid (99%) (TFA) (Acros), triisopropylsilane (99%) (TIPS) (Acros), ethyl ether (Fisher Scientific), dithiothreitol (DTT) (Acros), potassium hydroxide (KOH) (EM Science), L-cysteine hydrochloride monohydrate (MP Biomedical), *N*-methylmorpholine (NMM) (Fisher Scientific), *N*-methylpyrrolidone (NMP) (Fisher Scientific), gluteraldehyde (25%) (Sigma), concentrated HNO_3 (Sigma), concentrated HCl (Sigma), Ellman's reagent (bis(4-nitro-5-carboxylphenyl)disulfide) (Pierce), tris(hydroxymethyl)aminomethane hydrochloride (Fisher Scientific) and piperidine (99%) (Fisher Scientific).

2.2. Peptide synthesis

A peptide consisting of $PLCys_n$ ($n = 20$) was synthesized on Wang resin by Fmoc-solid phase peptide synthesis using a Ranin Symphony Quartet automated peptide synthesizer. Cleavage protocols have been described earlier [30]. The purity of the sequence was found to be 87% as determined by reverse phase-HPLC. No other single component was in excess of 5%.

2.3. Immobilization of $PLCys_n$ onto γ-Fe_2O_3 nanoparticles

γ-Fe_2O_3 nanoparticles with diameters of 5–25 nm (surface area 50–245 m^2 g^{-1}) were purchased from Sigma–Aldrich (iron(III) oxide nanopowder). Modification of 0.1 g γ-Fe_2O_3 nanoparticles with 3-aminopropyltriethoxysilane (3-APS) was carried out according to a procedure by Iida et al. (**I**) [31]. After modification, the particles were rinsed with copious amounts of water and dried under N_2. $PLCys_n$ attachment using a gluteraldehyde linkage was then carried out following a procedure originally published by Masoom and Townshend [32]. The 3-APS-modified particles were allowed to react with 5% gluteraldehyde in a 0.01 M phosphate buffer (pH 8.0) under N_2 for 90 min at room temperature (**II**). The gluteraldehyde serves as a linker between the amine terminus on the 3-APS and the amine terminus of the $PLCys_n$. Once the gluteraldehyde was attached, the nanoparticles were rinsed with water. $PLCys_n$ then was dissolved in 0.01 M phosphate buffer (pH 8.5) and allowed to react with ~10 mg of gluteraldehyde-modified γ-Fe_2O_3 nanoparticles for 2 h at room temperature under N_2 (**III**). The following equations show the steps leading to the immobilization of $PLCys_n$ on γ-Fe_2O_3 nanoparticles:

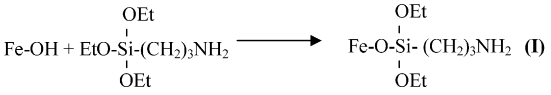

(1)

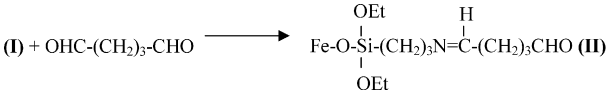

(2)

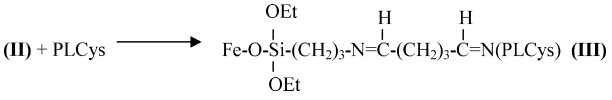

(3)

2.4. Instrumentation

The attachment of 3-APS groups to the surface of the γ-Fe_2O_3 nanoparticles and the linking of $PLCys_n$ were validated using a

Fourier transform infrared spectrometer (FTIR) (JEOL JIR-WINSPEC 50). A KBr pellet containing the sample was used for the FTIR spectroscopic measurements, and the spectra were collected between 400 and 4200 cm^{-1}.

A quantitative Ellman's test [33] using an Agilent 8453 UV–vis spectrophotometer was used to determine the number of thiol functionalities on the surface of the γ-Fe_2O_3 nanoparticles after functionalization.

Determinations of metal concentrations were carried out on an inductively coupled plasma time-of-flight mass spectrometer (ICP-MS) (Optimass 8000, GBC Scientific, Hampshire, IL). The ICP-MS was optimized for normal operating conditions of 1.2 kW forward power, 1 mL/min sample delivery rate and 1 L/min nebulizer gas flow rate.

2.5. Metal binding characteristics of PLCys–Nano and unfunctionalized γ-Fe_2O_3

2.5.1. Binding of metals to PLCys–Nano

Prior to metal binding, the PLCys–Nano were rinsed in 0.02 mol L^{-1} DTT in 0.02 mol L^{-1} of HEPES buffer (pH 8.0) in order to reduce disulfide bonds that may have formed between cysteine groups. The DTT solution was deaerated with N_2 prior to use and the reaction was allowed to proceed under constant mixing for 1 h. The PLCys–Nano were then collected using a neodymium–boron (Nd–B) magnet (3 mm × 3 mm × 3 mm) that produced an inhomogeneous magnetic field (0.37 T on the surface of the magnet). 0.5 mg PLCys–Nano were added to 100 mL of a deaerated metal solution consisting of 1000 $\mu g\,L^{-1}$ metal in 0.02 mol L^{-1} HEPES buffer (pH 7.0). The metals examined were As(III), Cd(II), Cu(II), Ni(II), Pb(II) or Zn(II). The PLCys–Nano were dispersed in solution using sonication and allowed to react in the metal solution. After collection using the Nd–B magnet, the final metal concentration of the reaction solution was determined using ICP-MS. All metal standards were prepared in 0.02 mol L^{-1} HEPES, and all studies were repeated with the unfunctionalized γ-Fe_2O_3 nanoparticles as a comparison.

The efficiency of metal extraction was also evaluated. After exposure to metal solution, PLCys–Nano were rinsed with 5 mL 0.02 mol L^{-1} HEPES to remove any weakly adsorbed metal. This rinse was also analyzed by ICP-MS. The particles were then dispersed in a 0.1 mol L^{-1} HNO_3 solution and allowed to react for 5 min while stirring. The extracting solution was then analyzed by ICP-MS after the nanoparticles were magnetically removed from the solution. Metal standards for the extraction experiments were prepared in both 0.02 mol L^{-1} HEPES and 0.1 mol L^{-1} HNO_3.

2.5.2. Evaluation of conditional stability constants

Using batch analysis, conditional stability constants were calculated for each metal at pH 7.0. After thiol reduction by DTT, 1.0 mg of PLCys–Nano were exposed to a 100 $\mu g\,L^{-1}$ As(III), Cd(II), Cu(II), Ni(II), Pb(II) or Zn(II) solution. After 5 min, the PLCys–Nano were collected using the Nd–B magnet, and the metal concentration of the solution was determined using ICP-MS. The concentration was raised by 100 $\mu g\,L^{-1}$ increments until metal binding had plateaued. From this data, conditional stability constants were calculated using Graphpad Prism 5®.

2.5.3. pH studies

The effect of varying pH conditions on PLCys–Nano metal binding was also determined. 0.5 mg of reduced PLCys–Nano were exposed to 1 mg L^{-1} As(III), Cd(II), Cu(II), Ni(II), Pb(II) and Zn(II) solutions at pH 4.0, 5.0, 6.0, 7.0, 8.0 and 9.0. After 5 min of exposure, the metal concentration of the solution was determined by ICP-MS.

3. Results and discussion

3.1. Immobilization of $PLCys_n$ onto γ-Fe_2O_3 nanoparticles

FTIR spectra of unfunctionalized γ-Fe_2O_3 nanoparticles, 3-APS-modified γ-Fe_2O_3 nanoparticles and PLCys–Nano are shown in Fig. 2. A broad absorption band in the range from 900 to 1100 cm^{-1} observed in the FTIR spectrum (b) of the 3-APS-modified γ-Fe_2O_3 nanoparticles can be attributed to Si–O stretching [34]. The 3-APS-modified γ-Fe_2O_3 nanoparticles also possess absorption bands in 1096.9 and 1010.1 cm^{-1} due to Si–O–Si and Si–O–Fe bonds [35–37], bands at 2918.6 and 2960.8 cm^{-1} due to stretching vibration of C–H bond and 799.3 cm^{-1} due to the bending vibration of $-NH_2$ group [34]. All these confirm that 3-APS was present and chemically bound to the surface of the nanoparticles. The immobilization of $PLCys_n$ on the surface of the γ-Fe_2O_3 nanoparticles is also suggested in spectrum (c) by the presence of S–H absorption band in 2575 cm^{-1} [34].

More convincing evidence of the immobilization of $PLCys_n$ to the surface of the nanoparticles was provided by the quantitative Ellman's test. Analysis of the PLCys–Nano revealed sulfur content of 53 (±1) μmol S per g of γ-Fe_2O_3 nanoparticles. This corresponds to a surface coverage of *ca.* 10^{15} $PLCys_n$ residues/cm^2 γ-Fe_2O_3 nanoparticles, assuming a surface area of 147.5 m^2/g γ-Fe_2O_3 nanoparticles (the median value for the range provided by Sigma–Aldrich). While this surface coverage is larger than one might expect for a molecule the size of $PLCys_n$, it is possible that the size of the particle and the accompanying small radius of curvature permit coverages in excess of what might be expected with a flatter surface. We did not perform BET or similar measurements on these particles, and an exact explanation for this observation is not known at this time.

Both PLCys–Nano and the unfunctionalized γ-Fe_2O_3 nanoparticles were exposed to a solution of 4 mol L^{-1} HCl in order to examine whether the $PLCys_n$ coverage was sufficient to protect the base ferric oxide particle. The solution containing the *unfunctionalized* γ-Fe_2O_3 nanoparticles turned bright yellow immediately, indicating that the nanoparticles had dissolved resulting in the formation of iron(III) chloride. The PLCys–Nano never dissolved, even after 48 h of exposure to the acid solution. Thus, the coverage of the immobilized $PLCys_n$ must be sufficient to prevent attack of the acid on the iron oxide particle, viz., suggestive of near monolayer coverage. This experiment also suggests the possible use of the modified nanoparticles in harsher chemical environments than might have been possible with the uncoated particle. This would allow the use

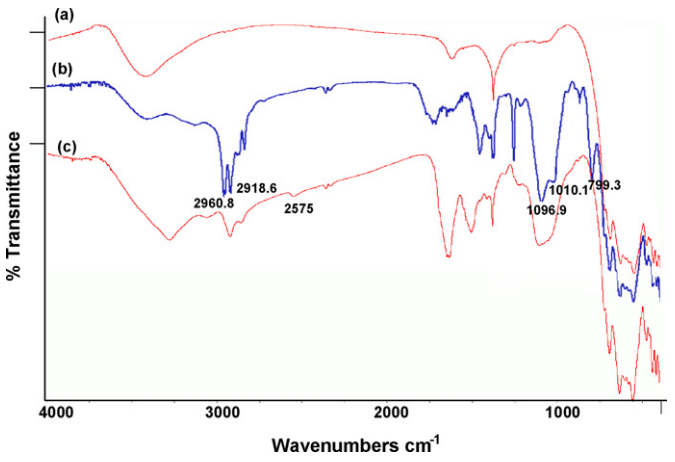

Fig. 2. FTIR spectra for: (a) as-received unfunctionalized γ-Fe_2O_3 nanoparticles; (b) 3-APS-modified γ-Fe_2O_3 nanoparticles; (c) functionalized PLCys–Nano. Hash marks on *y*-axis indicate 100% transmittance for each spectrum.

Table 1
Metal-binding capacities on PLCys–Nano and unfunctionalized γ-Fe_2O_3 nanoparticles as determined by ICP-MS

Metal ion	Capacity (μmol metal/g Fe_2O_3) on PLCys–Nano	Capacity (μmol metal/g Fe_2O_3) on unfunctionalized γ-Fe_2O_3	Enhancement factor[a]
As(III)	341 ± 58	164 ± 35	2
Cd(II)	385 ± 36	491 ± 15	0.8
Cu(II)	681 ± 19	522 ± 39	1.3
Ni(II)	559 ± 34	316 ± 32	1.8
Pb(II)	71 ± 12	90 ± 8	0.8
Zn(II)	368 ± 22	317 ± 15	1.2

50 mmol L^{-1} HEPES, pH 7.0, triplicate measurements. Uncertainties expressed as sample standard deviations, reflect measurement uncertainties only.
[a] Ratio of metal capacity of PLCys–Nano to metal capacity of unfunctionalized γ-Fe_2O_3.

of acid rinse for reclamation of metals from the particles, and further suggests longer lifetime and greater cost effectiveness since the media can be fully recovered.

3.2. Metal binding studies of PLCys–Nano

3.2.1. Determination of reaction time

The length of time PLCys–Nano exposed to metal solution was varied from 2.5 to 10 min in order to determine appropriate reaction times. The amounts of metal uptake for all exposure times were found to be statistically similar, indicating that binding occurs in ≤2.5 min. This result is not unexpected due to the relatively high particle density alluded to earlier combined with the previous studies of Stair and Holcombe [38] that suggested rapid metal–peptide binding kinetics. Additionally, metal diffusion was expected to be fast as it is only limited by the amount of time it takes to reach the nanoparticles, which are present in relatively high density (ca. 3×10^7 cm^{-3}). This is an advantage over other common, macroscopic porous solid supports such as modified polymer resin beads, porous glass, etc. where effective particle density in solution is considerably lower in batch extractions and even after analyte diffuses to the media, slower diffusion to the interior binding sites can require additional time.

3.2.2. Binding of metals to PLCys–Nano

The PLCys–Nano and unfunctionalized γ-Fe_2O_3 nanoparticles binding/adsorption capacities were obtained for As(III), Cu(II), Cd(II), Ni(II), Pb(II) and Zn(II) at pH 7.0 and the results are shown in Table 1. PLCys–Nano displays large binding capacities for all of the metals tested; and in the case of As(III), Cu(II), Ni(II) and Zn(II), these capacities are larger than adsorption capacities obtained for the unfunctionalized γ-Fe_2O_3 nanoparticles. Additionally, the uptake of all the metals tested based on a per gram basis is over an order of magnitude greater than previous results with $PLCys_n$ immobilized onto control pore glass and glassy carbon electrodes [9–11,14], probably due to the larger surface area of the γ-Fe_2O_3 nanoparticles. Metal adsorption capacities over an order of magnitude greater than those observed in this study have been obtained for unfunctionalized iron oxide nanoparticles in other studies [24,39–41], but metal exposure times were longer (up to 24 h) and different iron oxide forms and crystal structures were used. The exposure times for both the functionalized and unfunctionalized particles were kept the same in this study in order to make a fair comparison, but longer metal exposure times may result in better adsorption to the unfunctionalized particles for some metals.

Using the $PLCys_n$ coverage value determined by Ellman's test, metal-to-$PLCys_n$ ratios were calculated for each metal. The ratios were 2.8 ± 0.5 As(III)/chain, 3.2 ± 0.3 Cd(II)/chain, 5.7 ± 0.2 Cu(II)/chain, 4.7 ± 0.3 Ni(II)/chain, 0.6 ± 0.1 Pb(II)/chain and 3.1 ± 0.2 Zn(II)/chain. These ratios are very similar to those obtained in previous studies with $PLCys_n$ immobilized onto glass and glassy carbon electrodes [9–11,14].

The functionalized and unfunctionalized nanoparticles also exhibit different metal affinities, which is to be expected due to the metal selectivity of $PLCys_n$. PLCys–Nano had a binding trend of Cu(II) > Ni(II) > Cd(II) ~ Zn(II) ~ As(III) > Pb(II). This trend, with the exception of Pb(II) and Ni(II), closely corresponds with typical soft acid metal binding preferences that are expected of a soft acid base such as a thiol [13]. The unfunctionalized γ-Fe_2O_3 nanoparticles had an adsorption trend of Cu(II) > Cd(II) > Ni(II) ~ Zn(II) > As(III) > Pb(II). This trend is surprising since both As(III) and Pb(II) are known to adsorb well to iron oxide. As was previously mentioned, a longer metal exposure time may result in better adsorption for some metals and therefore change the observed trend.

Previous studies conducted with $PLCys_n$ have shown that metals can be quantitatively recovered by simply lowering the pH, which induces a tertiary structure change in the peptide. Metal recoveries obtained after sonicating PLCys–Nano in 5 mL of a 0.1 mol L^{-1} HNO_3 solution for 5 min are shown in Table 2. Good metal recoveries were observed for Ni(II), while poorer recoveries were seen for the other metals (Cd(II), Cu(II), Pb(II) and Zn(II)). Very poor recoveries were observed for As(III). In a study by Howard et al., it was determined that $PLCys_n$ contains both strong and weak sites for Cd(II), Cu(II) and Pb(II), while almost no strong sites were observed for Ni(II) [11]. It is reasonable to believe that the Cd(II), Cu(II) and Pb(II) not recovered are bound to strong binding sites within the $PLCys_n$. As(III) has been shown to bind strongly ($\log K > 16$) and irreversibly to cysteine containing proteins [42,43] which may explain why very little recovery was observed. Additionally, Compton and co-workers also experienced irreversible As(III) binding to immobilized $PLCys_n$ on glassy carbon microspheres [44].

3.3. Evaluation of conditional stability constants

Using batch equilibrium analysis, binding information was obtained for PLCys–Nano based on a one-site binding model. Using Graphpad Prism 5®, conditional stability constants were calculated for each metal. From a fit of the data, the estimated $\log K$ is 4.5 for As(III), 4.1 for Cd(II), 5.2 for Cu(II), 5.2 for Ni(II), 5.9 for Pb(II) and 6.5 for Zn(II). The values obtained for Cd(II) and Cu(II) are consistent with the ranges previously reported for $PLCys_n$ immobilized onto CPG [10,11].

Table 2
Metal recovery for PLCys–Nano

Metal ion	Recovery (%)
As(III)	22 ± 8
Cd(II)	71 ± 9
Cu(II)	60 ± 20
Ni(II)	89 ± 15
Pb(II)	67 ± 4
Zn(II)	50 ± 10

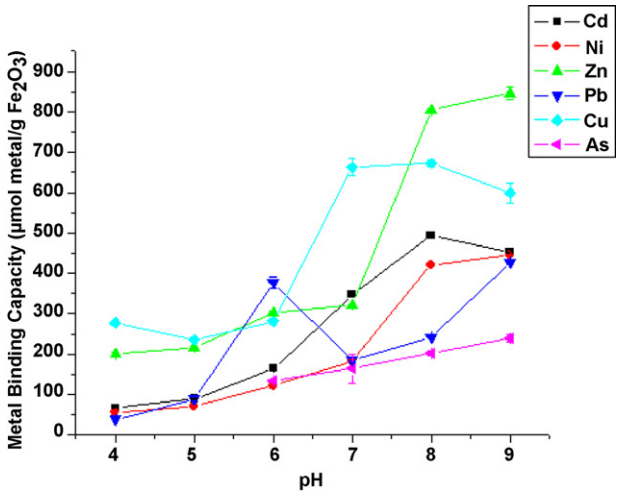

Fig. 3. Effect of pH on PLCys–Nano binding. All measurements were made in triplicate and uncertainties are reported as standard deviations. As(III) values for pH 4 and 5 were not significantly detectable above blank levels and are omitted.

3.4. pH studies

The effect of changing pH on PLCys–Nano binding was also evaluated and these results are shown in Fig. 3. As expected, more metal bound with increasing pH, likely due to the deprotonation of PLCys$_n$'s thiol moieties. While optimal binding is at pH $\geq$ 7.0, metal binding is observed over a wide pH range illustrating the particles' effectiveness.

4. Conclusions

PLCys$_n$ has been successfully immobilized onto magnetic γ-Fe_2O_3 nanoparticles (PLCys–Nano) and been demonstrated as an inexpensive and novel heavy metal chelator. The use of magnetic particles with a chelator "coating" is attractive since such a system can provide fast and efficient recovery of the metal chelating system following their use in bulk extractions from solutions. Additionally, the PLCys–Nano provided metal selectivity over the unfunctionalized particles. The reported approach is easily adapted to the attachment of other peptide chelators which may exhibit selectivity for other groups of targeted metals.

The PLCys–Nano exhibited metal binding capacities over an order of magnitude larger than traditional supports, perhaps due to the high density of particles in solution and the larger number of metal binding sites on the *surface* of the support. PLCys–Nano also exhibited rapid metal uptake ($\leq$2.5 min) and had larger metal capacities than unfunctionalized γ-Fe_2O_3 nanoparticles for several metals. Using a simple acid solution, metal recoveries of >50% were obtained for all of the metals except As(III). Due to the protective character of the PLCys$_n$ monolayer on the γ-Fe_2O_3 nanoparticles, dissolution of the nanoparticles was minimal when exposed to acidic solutions that typically attacked the iron oxide particles.

PLCys$_n$, which has a general metal selectivity towards soft metals acids, was chosen to demonstrate the proof of concept. Greater metal selectivity may be achievable through the use of combinatorial peptide library screening or by using peptide fragments based on known metal binding proteins.

Acknowledgements

This work was supported, in part, by the Robert A. Welch Foundation and the Texas Hazardous Waste Research Center. We would like to thank Professor C. Grant Wilson for use of the FTIR spectrometer and Klaus Linse, Sandra Smith and Michelle Gadush for their assistance in peptide synthesis. BTS also gratefully acknowledges the support of a University of Texas Co-Op Undergraduate Fellowship.

References

[1] L. Jarup, Hazards of heavy metal contamination, Br. Med. Bull. 68 (2003) 167–182.
[2] M.P. Ireland, Biological Monitoring of Heavy Metals, John Wiley & Sons, New York, 1991.
[3] J.P. Vernet, Impact of Heavy Metals on the Environment, Elsevier, New York, 1992.
[4] L. Malachowski, J.L. Stair, J.A. Holcombe, Immobilized peptides/amino acids on solid supports for metal remediation, Pure Appl. Chem. 76 (2004) 777–787.
[5] B. Anderson, Evaluation of immobilized metallothionein for trace metal separation and preconcentration, Dissertation, The University of Texas at Austin, Austin, TX, p. 215.
[6] L.H. Chen, C.S. Chung, Steric and macrocyclic effects in the dissociation kinetics of cyclic and open-chain tetraamine complexes of copper(II) in strongly acidic, aqueous media, Inorg. Chem. 27 (1988) 1880–1885.
[7] T.C. Miller, E.S. Kwak, M.E. Howard, D.A. Vanden Bout, J.A. Holcombe, An in situ study of metal complexation by an immobilized synthetic biopolymer using tapping mode liquid cell atomic force microscopy, Anal. Chem. 73 (2001) 4087–4095.
[8] H. Autry, J.A. Holcombe, Cadmium, copper and zinc complexes of poly-L-cysteine, Analyst 120 (1995) 2643–2647.
[9] H.A. Jurbergs, J.A. Holcombe, Characterization of immobilized poly(L-cysteine) for cadmium chelation and preconcentration, Anal. Chem. 69 (1997) 1893–1898.
[10] M.E. Howard, H.A. Jurbergs, J.A. Holcombe, Effects of oxidation of immobilized poly(L-cysteine) on trace metal chelation and preconcentration, Anal. Chem. 70 (1998) 1604–1609.
[11] M.E. Howard, H.A. Jurbergs, J.A. Holcombe, Comparison of silica-immobilized poly(L-cysteine) and 8-hydroxyquinoline for trace metal extraction and recovery, J. Anal. Atom. Spectrom. 14 (1999) 1209–1214.
[12] G.G. Wildgoose, H.C. Leventis, I.J. Davies, A. Crossley, N.S. Lawrence, L. Jiang, T.G.J. Jones, R.G. Compton, Graphite powder derivatised with poly-L-cysteine using "building block" chemistry—a novel material for the extraction of heavy metal ions, J. Mater. Chem. 15 (2005) 2375–2382.
[13] F.A. Cotton, G. Wilkinson, Advanced Inorganic Chemistry: A Comprehensive Text, 4th ed., John Wiley & Sons, New York, 1980.
[14] A.M. Johnson, J.A. Holcombe, Poly(L-cysteine) as an electrochemically modifiable ligand for trace metal chelation, Anal. Chem. 77 (2005) 30–35.
[15] S.M.C. Ritchie, D. Bhattacharyya, Membrane based hybrid processes for high water recovery and selective inorganic pollutant separation, J. Hazard. Mater. 92 (2002) 21–32.
[16] S.M.C. Ritchie, K.E. Kissick, L.G. Bachas, S.K. Sikdar, C. Parikh, D. Bhattacharyya, Polycysteine and other polyamino acid functionalized microfiltration membranes for heavy metal capture, Environ. Sci. Technol. 35 (2001) 3252–3258.
[17] S.C. Chang, T.I. Anderson, S.E. Bahrman, C.L. Gruden, A.I. Khijiniak, P. Adriaens, Comparing recovering efficiency of immunomagnetic separation and centrifugation of mycobacteria in metalworking fluids, J. Ind. Microbiol. Biotechnol. 32 (2005) 629–638.
[18] J.J. Hubbuch, D.B. Matthiesen, T.J. Hobley, O.R.T. Thomas, High gradient magnetic separation versus expanded bed adsorption: a first principle comparison, Bioseparation 10 (2001) 99–112.
[19] B.L. Hirschbein, D.W. Brown, G.M. Whitesides, Magnetic separations in chemistry and biochemistry, Chemtech. 12 (1982) 172–179.
[20] H. Tamura, R. Furrichi, Adsorption affinity of divalent heavy metal ions for metal oxides evaluated by modeling with the Frumkin isotherm, J. Colloid Interf. Sci. 195 (1997) 241–249.
[21] S.E. Ziemniak, L.M. Anovitz, M.L. Machesky, P. Benezeth, D.A. Palmer, Solubility and surface adsorption characteristics of metal oxides, in: D.A. Palmer, R. Fernandez-Prini, A.H. Harvey (Eds.), Aqueous Systems at Elevated Temperatures and Pressures, Elsevier, London, 2004, pp. 493–595.
[22] R.M. McKenzie, The adsorption of lead and other heavy metals on oxides of manganese and iron, Aust. J. Soil Res. 18 (1980) 61–73.
[23] D.A. Clifford, G.L. Ghurye, Metal-oxide adsorption, ion exchange, and coagulation-microfiltration for arsenic removal from water, in: W.T. Frankenberger Jr. (Ed.), Environmental Chemistry of Arsenic, Marcel Dekker, Inc., New York, 2002, pp. 217–245.
[24] C.T. Yavuz, J.T. Mayo, W.W. Yu, A. Prakash, J.C. Falkner, S. Yean, L. Cong, H.J. Shipley, A. Kan, M. Tomson, D. Natelson, V.L. Colvin, Low-field magnetic separation of monodisperse Fe_3O_4 nanocrystals, Science 314 (2006) 964–967.
[25] S. Dixit, J.G. Hering, Comparison of As(V) and As(III) sorption onto iron oxide minerals: implications for arsenic mobility, Environ. Sci. Technol. 37 (2003) 4182–4189.
[26] J.F. Ferguson, J. Gavis, A review of the arsenic cycle in natural waters, Water Res. 6 (1972) 1259–1274.

[27] C.K. Jain, I. Ali, Arsenic: occurrence, toxicity and speciation techniques, Water Res. 34 (2000) 4304–4312.
[28] S. Li, Y. Chen, B.P. Rosen, Role of vicinal cysteine pairs in metalloid sensing by the ArsD As(III)-responsive repressor, Mol. Microbiol. 41 (2001) 687–696.
[29] W. Shi, J. Dong, R.A. Scott, M.Y. Ksenzenko, B.P. Rosen, The role of arsenic–thiol interactions in metalloregulation of the ARS operon, J. Biol. Chem. 271 (1996) 9291–9297.
[30] B.R. White, J.A. Holcombe, Fluorescent peptide sensor for the selective detection of Cu^{2+}, Talanta 71 (2007) 2015–2020.
[31] H. Iida, T. Nakanishi, T. Osaka, Surface modification of Fe_2O_3 nanoparticles with aminopropylsilyl groups and interparticle linkage with dicarboxylic acids, Electrochim. Acta 51 (2005) 855–859.
[32] M. Masoom, A. Townshend, Determination of glucose in blood by flow injection analysis and an immobilized glucose oxidase column, Anal. Chim. Acta 166 (1985) 111–118.
[33] G.L. Ellman, Tissue sulfhydryl groups, Arch. Biochem. Biophys. 82 (1959) 70–77.
[34] D.R. Lide (Ed.), CRC Handbook of Chemistry and Physics, 83rd ed., CRC Press, 2002.
[35] O.M. Mikhailik, O.M. Fedorenko, S.S. Mikhailova, V.I. Povstugar, A.M. Lyakhovich, G.T. Kurbatova, N.I. Shklovskaya, A.A. Chuiko, Surface structure of finely dispersed iron powders. III. Structure of a aminopropyltriethoxysilane-modified coating, Colloids Surf. 52 (1991) 331–338.
[36] K. Wapner, G. Grundmeier, Spectroscopic analysis of the interface chemistry of ultra-thin plasma polymer films on iron, Surf. Coat. Technol. 200 (2005) 100–103.
[37] Z. Xu, Q. Liu, J.A. Finch, Silanation and stability of 3-aminopropyl triethoxy silane on nanosized suparamagnetic particles. I. Direct silanation, Appl. Surf. Sci. 120 (1997) 269–278.
[38] J.L. Stair, J.A. Holcombe, Metal remediation and preconcentration using immobilized short-chain peptides composed of aspartic acid and cysteine, Microchem. J. 81 (2005) 69–80.
[39] S.R. Kanel, B. Manning, L. Charlet, H. Choi, Removal of arsenic(III) from groundwater by nanoscale zero-valent iron, Environ. Sci. Technol. 39 (2005) 1291–1298.
[40] S. Yean, L. Cong, C.T. Yavuz, J.T. Mayo, W.W. Yu, A. Kan, V.L. Colvin, M. Tomson, Effect of magnetite particle size on adsorption and desorption of arsenite and arsenate, J. Mater. Res. 20 (2005) 3255–3264.
[41] R.R. Gadde, H.A. Laitinen, Studies of heavy metal adsorption by hydrous iron and manganese oxides, Anal. Chem. 46 (1974) 2022–2026.
[42] S. Silver, G. Ji, S. Broer, S. Dey, D. Dou, B.P. Rosen, Orphan enzyme or patriarch of a new tribe: the arsenic resistance ATPase of bacterial plasmids, Mol. Microbiol. 8 (1993) 637–642.
[43] N.A. Rey, O.W. Howarth, E.C. Pereira-Maria, Equilibrium characterization of the As(III)–cysteine and the As(III)–glutathione systems in aqueous solution, J. Inorg. Biochem. 98 (2004) 1151–1159.
[44] G.G. Wildgoose, H.C. Leventis, A.O. Simm, J.H. Jones, R.G. Compton, Electrocatalysis at graphite and carbon nanotube modified electrodes: edge-plane and tube ends are the reactive sites, Chem. Commun. 7 (2005) 829–841.